SPECIAL FOCUS:
NON-BUILDING STRUCTURES

Seismic Design and Response of Crane-Supporting and Heavy Industrial Steel Structures

JULIEN RICHARD, SANDA KOBOEVIĆ and ROBERT TREMBLAY

ABSTRACT

This paper presents an analytical study of the seismic behavior of two different types of industrial buildings; a regular mill-type crane-supporting steel structure and an irregular heavy industrial building housing a vertical mechanical process. For both structures, the seismic response is examined through elastic time-history dynamic analyses in order to validate the predictions from the equivalent static force procedure and the response spectrum analysis method prescribed in current building codes. The analyses also serve to assess the inelastic demand in crane-supporting structure. For the crane-supporting structure, analyses are performed for sites in Montreal and Vancouver in Canada and in Seattle in the United States. The results show that the median horizontal displacement and acceleration from the time-history analyses are generally well predicted by the code analysis methods. Inelastic response in these buildings is likely to develop in the form of buckling of the lower column segment, a failure mode that exhibits limited ductility. For the tall irregular building, the analyses are performed for the Montreal site only. The results show the equivalent static method provides fair displacements estimate, but may lead to unconservative predictions of column and brace forces. Response spectrum analysis method, as prescribed in design codes, appears to provide appropriate prediction of the seismic response of such highly irregular structures. For both building types, a good prediction from response spectrum and time-history analysis methods is possible only when a sufficient number of modes are used.

Keywords: seismic design, crane structures, industrial buildings.

Industrial buildings house a wide variety of manufacturing, assembly, refining, mining or material handling processes, covering a broad range of products. They can also be part of critical facilities such as power plants and communication systems. Adequate seismic behavior is critical for these structures in order to shorten downtime periods that can cause substantial loss of revenues, unemployment or shortage of goods, electrical power and communication services. Industrial buildings may also serve for the production or storage of hazardous materials, and the unsatisfactory seismic structural response causing the leakage or malfunction can pose a major risk.

Steel-framed industrial buildings generally exhibited good overall structural performance in recent earthquakes. However, the reported structural damage to individual components or connections has resulted in disruption of operations in most of the industrial structures examined. Typical damage observed after the 1999 Kocaeli earthquake in Turkey included bolt shearing at column to roof truss connections in automotive plants, buckled and fractured braces, stretching and fracture of anchor bolts in moment-resisting frames, and shearing of anchor bolts (Bendimerad et al., 1999; Rahnama and Morrow, 2000; Sezen et al., 2000; Johnson et al., 2000). The 1994 Northridge earthquake caused yielding and failure of anchor bolts in an asphalt rock plant and brace buckling in a brewing facility (Tremblay et al., 1995). Failure of welds at brace connections was observed after the 1988 Spitak, Armenia, earthquake (Yanev, 1989). One steel-framed warehouse collapsed in the 1991 Costa Rica earthquake, but the cause was attributed to the overturning of the heavy building content against the steel columns (Swan and Hamburger, 1992). In the 1985 Chile earthquake (Thiel, 1986) and the 1989 Loma Prieta earthquake (Swan et al., 1990), buckling of braces and brace connection failures (sheared bolts, gusset plate buckling, and weld failures) occurred in various steel frames supporting equipments such as elevated tanks, cooling units and reactors.

Current code seismic design provisions in Canada and the United States have been essentially developed for conventional office or residential buildings that usually have regular and well-defined seismic force-resisting systems. The application of these provisions to industrial buildings that are typically characterized by complex and irregular geometries, uneven mass and/or stiffness distribution, and a large variety of dynamic properties is not straightforward for practicing engineers (Rolfes and MacCrimmon, 2007; Daali, 2004). In particular, there exist uncertainties regarding

Julien Richard, Structural Engineer, Hatch Engineering, Montreal, Quebec, Canada (corresponding author). E-mail: jrichard@hatch.ca

Sanda Koboević, Ph.D., Assistant Professor, Department of Civil, Geological and Mining Engineering, École Polytechnique, Montreal, QC, Canada. E-mail: sanda.koboevic@polymtl.ca

Robert Tremblay, Ph.D., Professor and Canada Research Chair in Earthquake Engineering, Department of Civil, Geological and Mining Engineering, École Polytechnique, Montreal, QC, Canada. E-mail: robert.tremblay@polymtl.ca

the amplitude and distribution of the seismic force and deformation demand on industrial structures. Furthermore, the highly ductile seismic force-resisting systems that have been introduced in codes in the last decades are not well suited for industrial applications. In order to achieve good inelastic performance and high energy dissipation capacity, these highly ductile systems rely on a carefully tailored lateral load path with balanced strength hierarchy, a condition that can hardly be maintained when mass or structural modifications are imposed over the years due to evolving production processes (e.g., addition of equipment or removal of braces or columns). Thus, for the sake of simplicity and flexibility, engineers typically prefer selecting conventional steel design and construction techniques, trading the simpler design and detailing for higher design seismic loads.

Both the National Building Code of Canada (NBCC) (NRCC, 2005) and the ASCE 7-05 code (ASCE, 2005) in the United States propose steel seismic force-resisting systems for which only limited or no special seismic detailing or capacity design verifications are required. Recognizing the inherent ductility of steel, it is permitted to design those simpler systems for seismic loads that are lower than the expected seismic elastic force level, i.e., using seismic force modification factors greater than 1.0: $R_d = 1.5$ in Canada, for the conventional construction category, and R between 3.0 and 3.5 in the United States, depending on the system used. Although these factors are much lower than those specified for the highly ductile systems (up to $R_d = 5.0$ in Canada and $R = 8.0$ in the United States), the solution may still be attractive in view of the lesser complexity in design and detailing and the greater flexibility for future modifications.

In moderate and high-seismicity zones, however, severe restrictions apply to buildings framed with these low-ductility systems. In Canada, the height of buildings designed with $R_d = 1.5$ is limited to 15 m (50 ft), recognizing the greater likelihood of localized high-ductility demand in taller structures subjected to seismic ground motions. In the United States, systems not specifically detailed for seismic resistance ($R = 3.0$) are not permitted in moderate and high seismic active zones, and only single-story structures with light roof dead loads are permitted up to 18.3 m (60 ft) if built with an ordinary braced steel frame ($R = 3.25$) or up to 20 m (65 ft) if ordinary moment-resisting frames ($R = 3.5$) are used. Typical industrial buildings often exceed these height limits, forcing the selection of highly ductile systems.

Exemptions or alternative design routes may apply to specific projects. For instance, the Commentary on NBCC (NRCC, 2005) specifies that the 15-m height restriction for $R_d = 1.5$ systems is intended to maintain the traditional three-story height limit imposed in previous NBCC editions and need not apply to single-story steel industrial structures such as steel mills, thus allowing low-ductility solutions to be adopted for these structures, regardless of their height. According to ASCE 7-05, relaxation of height limits is possible for ordinary braced frames and moment-resisting frames if the structure is designed as a nonbuilding structure, in accordance with requirements provided in Chapter 15. Unfortunately, it is not always clear in ASCE 7-05 under which circumstances an industrial building can be classified as a nonbuilding structure. Yet, this avenue may represent the only available option for tall industrial structures to be erected in moderate and high seismic zones.

Although the preceding limitations and exemptions generally make sense, there is very limited data on the seismic demand on industrial building steel structures under strong ground motions. Current system restrictions in codes have been essentially established from studies of the seismic performance of conventional office or residential buildings. It is, therefore, of the upmost importance to (1) gain a better knowledge of the seismic response of industrial buildings, (2) critically review existing design procedures, and (3) introduce seismic design provisions so that the intended performance can be achieved for these structures. The first step is necessary to support future actions, and the need for such data is becoming more pressing because changes are currently taking place in codes that will likely motivate the use of low-ductility systems for industrial buildings. In the upcoming 2010 edition of NBCC (Humar et al., 2010; Tremblay et al., 2010), it is proposed to increase the 15-m height limit for low-ductility steel frames, provided that minimum additional seismic requirements are implemented. In ASCE 7-10 (ASCE, 2010), precisions have been made in the definition of nonbuilding structures that allow for buildings housing equipment—with occupants involved only in the maintenance or monitoring of that equipment—to be considered as nonbuilding structures.

This paper describes the initial phase of an ongoing study investigating the seismic response of industrial buildings. The objective was to determine (1) if the analysis methods proposed in codes can adequately predict the actual force and deformation demand under seismic loads and (2) the location, extent and nature of the inelastic demand anticipated under strong ground motions from earthquakes. The study was carried out on selected industrial buildings designed according to the current building code provisions. Two building types were considered: (1) a regular crane-supporting steel structure typical of buildings found in the mill industry and (2) an irregular heavy industrial building housing a vertical mechanical process representative of mining and metal refining industry. In both cases, low-ductility seismic force resistant systems were assumed, even if that category was not permitted in current building codes, the intent being to obtain data that could be used to evaluate the relevance of current code restrictions. For the mill-type building, three different cities in North America (Montreal, Quebec; Vancouver, British Columbia; and Seattle, Washington) were considered to examine the influence of seismic hazard and ground motion characteristics on the structural response. For the Vancouver site, two different soil conditions were investigated. For the irregular heavy industrial building, the study was carried out for the Montreal site only. In all cases, elastic dynamic time-history analyses were conducted for selected acceleration records compatible with the design spectra at the site, and the results are were compared to those obtained from the static equivalent force procedure and the response spectrum analysis method prescribed in codes. For the irregular heavy industrial building, for which three-dimensional analysis was employed, attention is also given to the appropriate number of modes to use in response spectrum analysis and to the possible impact of the direction of seismic loading on member force demand.

DESIGN AND SEISMIC RESPONSE OF CRANE-SUPPORTING BUILDINGS

Building Geometry

A three-dimensional view of the crane-supporting structure studied is shown in Figure 1. The structure has a clear span of 25 m (82.0 ft) and consists of transverse moment-resisting frames that are regularly spaced 10 m (32.8 ft) on center to form a single crane aisle. Each frame includes a roof truss and simple columns that extend from fixed-base laced columns supporting both the roof and the crane runway girders (Figure 2). The truss-to-column connections are moment-resistant. The structure supports two 40-t (44-T) capacity overhead cranes. Horizontal loads acting along the longitudinal direction are resisted by horizontal X-bracing located at the roof level and by vertical X-bracing below and above the crane girders along the exterior walls. Typical steel siding supported on girts and purlins is used for the walls and the roof.

In this study, the seismic response of the transverse moment-resisting frames is examined, with particular attention directed to the crane-supporting columns. In view of the exploratory nature of the study, it was assumed for simplicity that lateral loads were resisted individually by each of the frames, thus omitting the possibility that part of the inertia loads induced by the crane weight be distributed to adjacent frames through the horizontal roof bracing. A two-dimensional numerical model of one transverse frame was therefore adopted for the design and analysis. For consistency with this assumption, a redundancy factor of 1.3 should have been considered in the seismic load calculation for the Seattle site, according to ASCE 7. This increase in seismic design loads was, however, ignored in this study to assess the actual seismic demand-to-capacity ratio without the bias introduced by the additional resistance required in ASCE 7 to compensate for the lack of redundancy. It was also assumed that the frame was located in the middle part of the aisle and was not a part of the longitudinal bracing system.

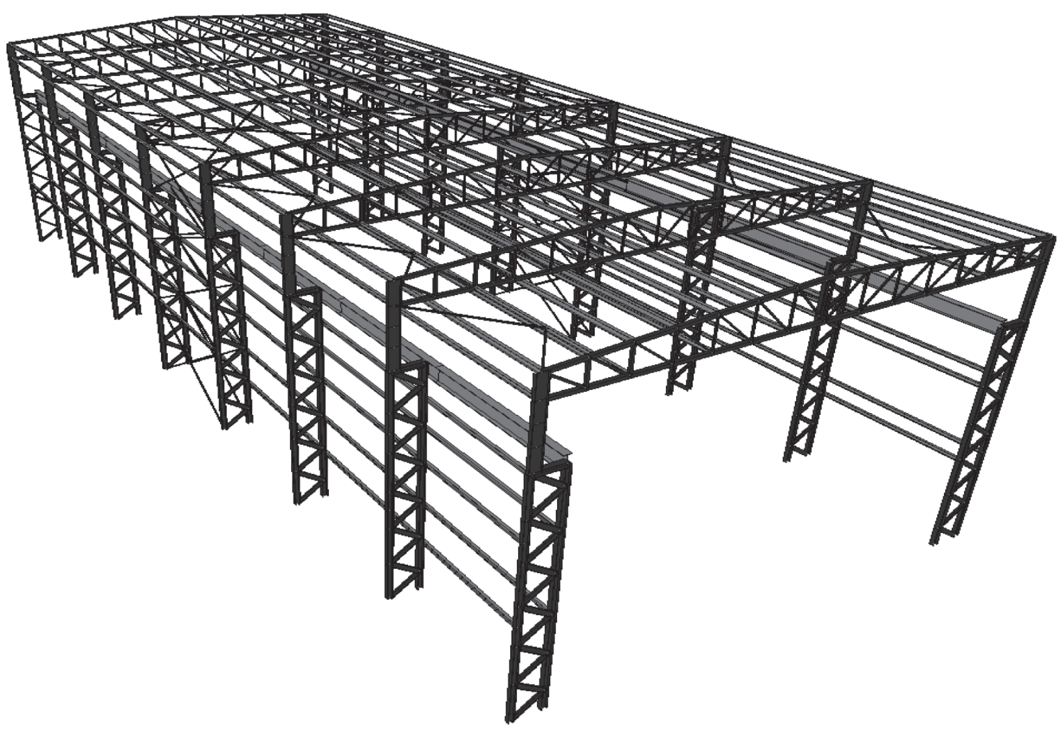

Fig. 1. Three-dimensional view of the crane-supporting building.

Parameter/Site	MTL-C	VAN-C	VAN-E	SEA-E
Total roof gravity load (S or L), kN (kips)	574 (129)	375 (84)	375 (84)	281 (63)
Total horizontal wind load, kN (kips)	211 (47)	256 (58)	256 (58)	187 (42)
T_1, s	1.34	1.25	1.20	1.21
T_2, s	0.21	0.23	0.26	0.21
T_3, s	0.10	0.10	0.10	0.10
M_1/M, %	89.0	87.5	87.3	87.5
M_2/M, %	2.6	2.9	3.0	3.1
M_3/M, %	4.5	5.4	5.5	5.2
W, kN (kips)	1230 (277)	1180 (265)	1190 (268)	1060 (238)
V, kN (kips)	71 (16)	176 (40)	333 (75)	146 (33)
V/W, %	5.8	14.9	28.0	13.8
V_t, kN (kips)	62 (14)	155 (35)	290 (65)	128 (29)
V_t/V	0.87	0.88	0.87	0.88
Steel tonnage, t	11.8	11.5	11.9	10.5

Table 1. Properties of the Crane-Supporting Structures (per frame)

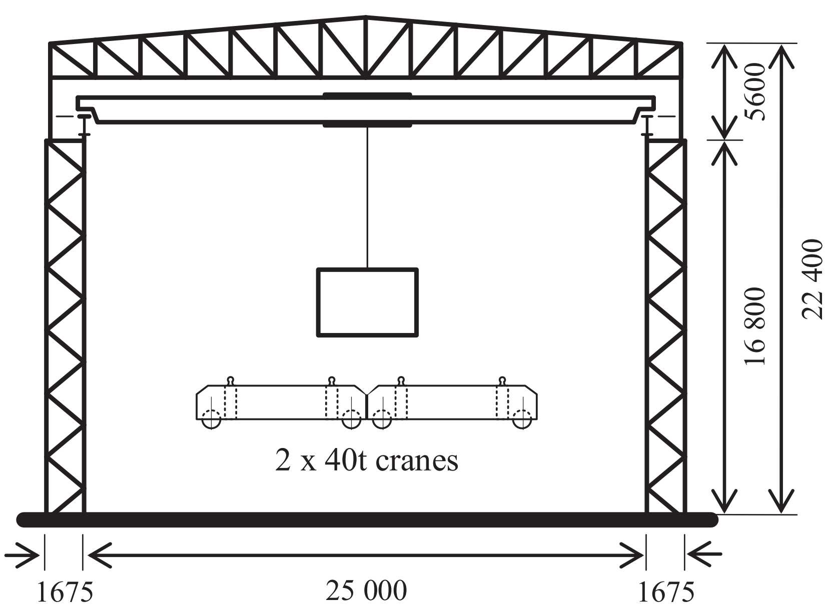

Fig. 2. Two-dimensional view of the frame studied (dimensions in mm).

Building Design

The structure was designed for four different sites: class C site in Montreal (MTL-C), class C and E sites in Vancouver (VAN-C and VAN-E), and class D site in Seattle (SEA-D). The designs were performed according to the applicable building codes at the sites: the 2005 National Building Code of Canada (NBCC) (NRCC, 2005) and the CAN/CSA-S16 (CSA, 2001) steel design standard for the Canadian locations and the ASCE 7-05 (ASCE, 2005) and the AISC *Specification* (AISC, 2005) for Seattle. All relevant loads and load combinations specified in codes were considered in the design. Roof snow loads of 1.96 kPa (40.9 psf) and 1.28 kPa (26.7 psf) were used for Montreal and Vancouver, respectively. In Seattle, the minimum roof live load of 0.96 kPa (20.0 psf) governed. The design guide for crane-supporting structures by MacCrimmon (2004) was consulted for the load combinations including crane induced loads as well as for the design of the runway girders. Deflection criteria were established according to AISE (2003) and Fisher (2004). Lateral deflections at the crane level under nonseismic loads were limited to the lesser of 50 mm (2.0 in) and $h/240$ (= 16,800 mm/240 = 70 mm = 2.8 in). Under seismic loads, the limit on total lateral deflections, including inelastic effects, at the crane and roof levels was taken as 2.5% of the respective heights, as recommended in buildings codes. Drift limits did not govern the design of any of the structures.

The design loads are summarized in Table 1. As required by NBCC, $1.0D + 0.25S$ (D = dead load, S = roof snow load) was included both in the calculation of seismic weight of the structure, W, and in the load combinations involving seismic loads. Vertical ground motion effects were not considered, as prescribed by NBCC. For the Seattle site, the seismic weight included dead load only, while $1.4D$ plus 50% of the roof live load was considered in the seismic load combinations. The factor 1.4 includes the ASCE 7 load factor of 1.2 and vertical acceleration effects (0.2). At all sites, the dead load of the two cranes, without lifted loads, was included in the seismic weight (or mass) as well as in the seismic load combinations. In this calculation, the two cranes were positioned longitudinally in the building to produce the most critical condition for the frame studied. Lateral loads from cranes were equally distributed to each side assuming double flanged wheels.

The elastic spectrum used for the seismic design at each site is shown in Figure 3. The fundamental periods obtained from modal analysis, T_1, are given in Table 1. For all cases, the T_1 value is close to or shorter than the upper limits on periods prescribed in codes for steel moment-resisting frames (in NBCC: $T \leq 1.5\ T_a = 1.5 \times 0.085h^{0.75}$ = 1.31 s, with h expressed in meters; in ASCE 7: $T \leq C_uT_a = 1.4 \times 0.028h^{0.8}$ = 1.22 s with h expressed in feet; where h = 22.4 m = 73.5 ft) and thus T_1 was used to determine the elastic spectral ordinates. The structures in Canada were assumed to be of the conventional construction (type CC) category. The total design lateral earthquake load or base shear, V, was obtained by dividing the elastic base shear, V_e, by R_dR_o, where R_d and R_o are the ductility- and overstrength-related force modification factors, respectively, with $R_d = 1.5$ and $R_o = 1.3$ ($R_dR_o = 1.95$). The base shear, V_e, is equal to $S(T_a)M_vIW$, where $S(T)$ is the design spectral acceleration at the period T, based on 2% probability of exceedance in 50 years, M_v is the higher mode adjustment factor, I is the importance factor, and W is the seismic weight. The design base shear V need not exceed two-thirds of the value of V

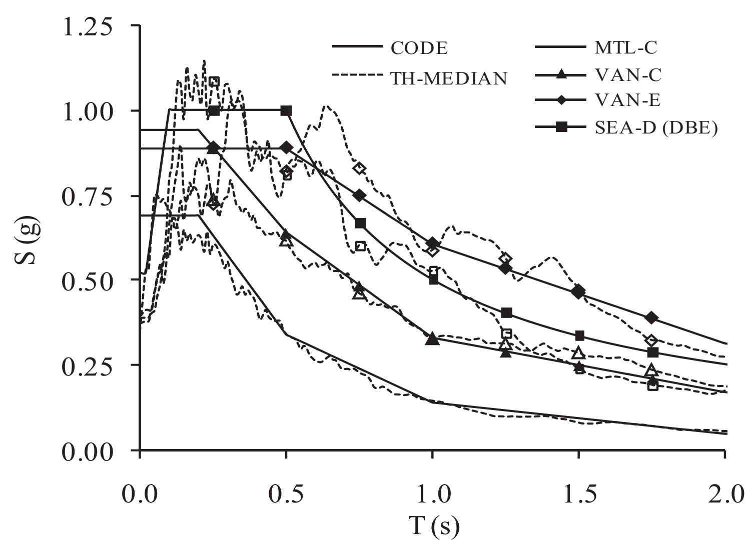

Fig. 3. Code design response spectra and median 5% damped acceleration spectra for the ground motion ensembles.

determined with $T = 0.2$ s. For Seattle, the design base shear $V = C_S W$, where $C_S = S_{D1}/T(R/I) < S_{DS}/(R/I)$ for the period range of the building studied. In the expression for C_S, S_{DS} and S_{D1} are the design spectral accelerations at short (0.2 s) and 1.0 s periods, respectively, and R is the force modification factor. The structure was designed as a building structure with $R = 3.0$ applicable to structures not explicitly detailed for seismic resistance. An importance factor $I = 1.0$ was adopted for all structures. The resulting values of V are presented in Table 1. Note that the building height exceeds the current 15-m (50-ft) limit prescribed for type CC systems in Canada, and an $R = 3.0$ system is not permitted for Seattle according to ASCE 7. As previously discussed, these code system restrictions were purposely ignored to examine their relevance.

Member forces and deflections for seismic design were determined using the modal response spectrum analysis method, and the modal contributions were combined using the complete quadratic combination (CQC) method, assuming 5% of critical damping in each mode. Member forces and deflections were also determined with the equivalent static force method for comparison purposes. In both methods, the total seismic weight (or mass) was distributed to every node of the structural model according to their tributary seismic weight (or mass). In the equivalent static method, the seismic lateral load V was distributed among the nodes based on the node heights and seismic weights in accordance with the applicable code vertical distribution procedure. For the response spectrum analysis, the results were divided by $R_d R_o$ or R, as applicable, and the resulting base shear force V_t was determined. The ratios V_t/V are presented in Table 1; the values are very consistent (0.87–0.88) and are all less than 1.0. Building codes require that the results from response spectrum analysis be scaled to avoid seismic forces much lower than the forces associated to the design earthquake force V. For the structures in Montreal and Vancouver, the response analysis results were scaled by the ratio V/V_t, as required in NBCC for irregular structures. For Seattle, V_t exceeds 0.85 V, and no calibration was required as per ASCE 7. Deflections from both analysis methods were multiplied by $R_o R_d = 1.95$, for the Canadian sites, and by the deflection amplification factor $C_d = 3.0$, for Seattle, to obtain deflection estimates including inelastic response effects.

Such a difference between V and V_t for a single-story building may seem counter-intuitive at first. It can be attributed to the fact that only two modes were considered in the modal combination to include up to 90% of the total structure mass, as prescribed in building codes. Table 1 gives the periods T_i and fraction of participating masses (M_i/M in %) for the first three lateral modes of vibration. The corresponding mode shapes are illustrated in Figure 4 for the MTL-C building. Higher modes with complex deformed shapes and substantial participating mass levels still exist in the structures, essentially because significant seismic weight is present at both the roof and crane levels (essentially the dead load of the cranes for the latter). Including a larger number of modes in the response spectrum analysis improves the prediction of the total seismic force. For instance, the base shear increases from 0.87 to 0.92 V for the MTL-C building when the contribution of the third mode of vibration is added, resulting in 96% total mass participation. Including additional modes has no further impact on the results, and the remaining difference between the static and response spectrum base shears arises from the inherent simplifying assumptions behind the equivalent static method. This effect is less pronounced when the cranes are not present in the frame bay studied, but this situation is less critical because the total seismic weight is reduced and the seismic loads are lower (by 30% and 15% on average, respectively, for the four buildings). Note that the response spectrum analysis results obtained for the case with the cranes present and considering only the first two modes of vibration, as prescribed in codes, are used herein for the discussion.

The columns are critical components of the seismic force-resisting system for these structures. For out-of-plane buckling, effective lengths were taken equal to the vertical distance between braced points, i.e., at third points between the base and the crane girder level for the laced column segment (at location of horizontal struts) and between the crane girder level and the truss bottom chord for the upper column segment. For in-plane buckling, the approach proposed by Schmidt (2001) was adopted. For each load combination,

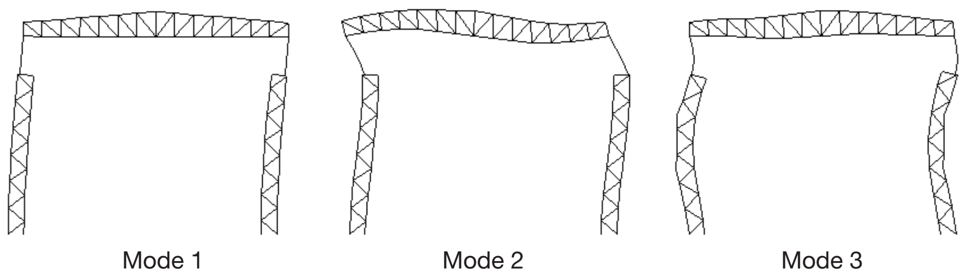

Fig. 4. First three lateral vibration modes for the MTL-C building (cranes not shown, but crane seismic weight included in analysis).

second-order analysis was performed, and horizontal notional loads equal to 0.5% of the gravity loads and acting in the same direction as the lateral loads were applied at the location where gravity loads were applied. For the seismic load combinations, second-order effects of gravity loads acting on the laterally displaced structure were determined by multiplying the first-order analysis results by the amplification factors given in CSA-S16 standard and ASCE 7 provisions. The notional loads account for the effects of initial out-of-plumbness and inelasticity and an effective length equal to the total column height (22.4 m = 73.5 ft) was adopted for both the upper and lower column segments. A K factor of 1.0 was used for bracing members, for both in-plane and out-of-plane buckling, as commonly done in design practice.

The upper column was oriented such that strong axis bending is in the plane of the frame. For that column segment, out-of-plane buckling about weak axis was critical in design. For the laced column segment, the interior and exterior columns were oriented such that in-plane buckling of the individual members occurs about the weak axis and the lacing members were assumed to be welded to the columns. The strength of the individual column members was determined using an equivalent slenderness accounting for the interaction between global and individual buckling modes, as specified in steel design standards. In-plane buckling of the individual column members at the column base governed the design of the interior and exterior columns.

After completion of the design, elastic buckling analysis was carried out for the VAN-C building to verify the effective slenderness ratios assumed in design for in-plane buckling of individual members. The verification was performed for different buckling modes and load combinations, and the cases where buckling mainly develops in the critical column members were identified. For these cases, the effective slenderness ratio of the member, KL/r, were obtained from the elastic buckling load equation: $(KL/r)^2 = \pi^2 EA/P_{cr}$, where $E = 200{,}000$ MPa (29,000 ksi), A is the cross-sectional area of the member and P_{cr} is the axial load carried by the member at buckling. In general, the slenderness ratios from analysis were smaller than the design values for the upper column segment and close to the design values for the individual column members at the base of the laced column segment. Figure 5a shows the frame global lateral buckling mode under dead, crane and wind loads. For this particular case, the KL/r value for the upper column is 73 from buckling analysis, compared to 105 assumed in design. Interaction between global and local buckling of the individual exterior column member at the base under the combination of dead, wind and snow loads is illustrated in Figure 5b. In this case, KL/r from analysis is 59 versus 63 in design. The slenderness ratios assumed in design were used later to evaluate the capacity of the members.

The required steel tonnage per frame is given in Table 1. Due to the relative importance of the crane loads, the final designs at the different sites were quite similar in spite of the differences between wind and seismic loads. In fact, for the Canadian sites, the seismic loads only governed the design of the upper column segment as well as the exterior column and lacing members of the laced column segment of the VAN-E frame. For Seattle, seismic load combinations were also critical for the upper column segment and the exterior column of the laced column segment, even if a higher force modification factor was used. This is partly due to the consideration of vertical seismic acceleration effects in design. In all other cases, crane or wind loads were critical except for the upper column segment of the frame in Montreal that was governed by roof snow load.

Validation of the Seismic Analysis Methods Used in Design

Elastic dynamic time-history analyses were carried out under sets of ground motions compatible with the design spectra to evaluate how successful the design procedures were in predicting the seismic-induced frame deformations and the distribution of seismic member forces. For each site, historical and simulated ground-motion time histories were selected based on magnitude–hypocentral distance scenarios that dominate the seismic hazard. A total of 14 records were

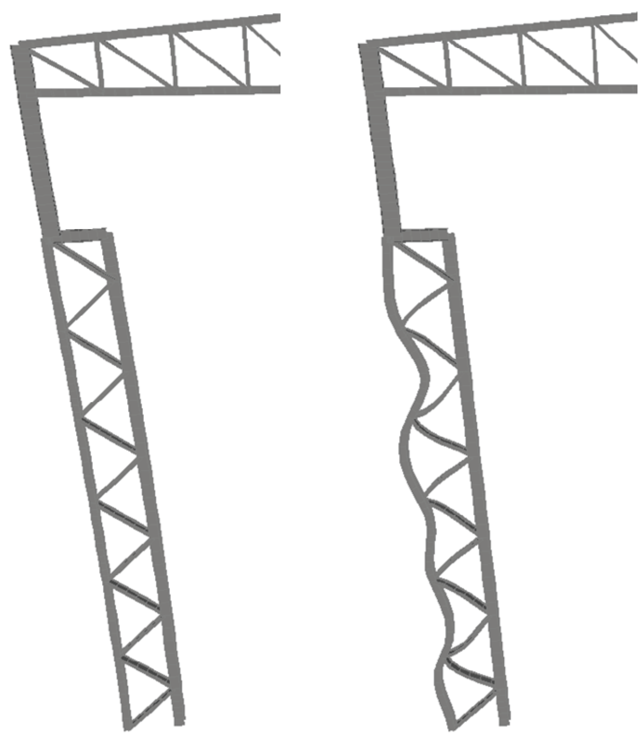

(a) *(b)*

Fig. 5. In-plane buckling modes of the frame: (a) global lateral buckling; (b) interaction between global lateral and individual exterior column buckling.

chosen for MTL-C, 24 for VAN-C, 12 for VAN-E and 20 for SEA-D. The records were scaled to represent the level of seismic loads considered in design. For Canadian locations, the calibration was done by matching the spectral intensities of the record and design spectrum at studied locations over the range of periods determined on basis of the best visual fit between the two spectra. For Seattle, the records available from the SAC database for that location were already calibrated for the appropriate site class and level of seismic hazard, and no additional scaling was needed. Detail of the ground motion selection and scaling can be found in Richard (2009). In Figure 3, the resulting median acceleration response spectra obtained for the four sites are compared to the corresponding design spectra. Time-history dynamic analysis was performed assuming 5% Rayleigh damping in the first two modes and the same seismic nodal masses as those used in design to ensure a consistent comparison.

The time-history analysis results are compared to the predictions from both the equivalent static force and response spectrum analysis methods. The response parameters examined are the peak lateral displacements and peak horizontal accelerations at the crane and roof levels, as well as the stress ratios for the upper column segment and for the individual exterior column member at the base of the laced column. These two column members were identified in design as the most critical under seismic load combinations, which was subsequently confirmed in the time-history analysis. For the column stress ratios, the force demand from time-history analysis was divided by R_dR_o or R, as applicable, and then combined with gravity load effects. The calculations were done using factored member resistances calculated with $\phi = 0.9$ and the nominal steel yield strength. The most critical results obtained from code interaction equations for the different possible failure modes (cross-section strength, in-plane flexural buckling and lateral-torsional buckling) were retained and compared to the corresponding stress ratios calculated for the seismic demand obtained from static and response analysis methods. For all response parameters, the peak values were first determined for each individual record, and the 50th and 84th percentile values were calculated for each ground-motion ensemble. Design procedures were evaluated on the basis of the median results, while the 84th percentile results are commented on to illustrate dispersion.

The total anticipated drift at the crane and roof levels, Δ_c and Δ_r, respectively, normalized by the height measured from the column base to each of the two locations, are shown in Figure 6. In all cases, displacement estimates obtained from the static and response spectrum analysis methods are similar, although the static values are generally slightly higher. The median values from time-history analysis are the smallest but still compare well with those obtained from static and response spectrum analyses. This similarity suggests that the first vibration mode dominated the displacement response. For the Vancouver frames, the 84th percentile values from time-history analysis exceed static analysis predictions, with the difference being more pronounced for Vancouver frame on soft soil (approximately 50%). The median displacements are all well below the limits adopted for seismic design. Note that ASCE 7-05 does not impose drift limits for single-story structures with flexible cladding, such as the structures examined in this study. However, with the exception of the Montreal site, the computed drifts do exceed the 50 mm (2.0 in) (0.30% *h*) limit that was considered in design for nonseismic load combinations to guard against the possible damage to the lifting equipment. In view of the importance of operational requirements for industrial buildings, it would be appropriate to include the limits on drifts computed at the crane level under seismic loads to prevent damage to the lifting equipment due to earthquakes.

In Figure 7, the results obtained for peak accelerations from response spectrum and time-history analysis are compared. With the exception of the VAN-E site, the median peak acceleration values from time-history analysis are equal or slightly smaller than those obtained from response spectrum analysis. For all cases, the difference between the 84th percentile and median values is less than 40%. For the Montreal frame, the computed accelerations at the crane level are larger than at the roof level, suggesting that higher modes were relatively more excited due to the high-frequency components of the ground motions in eastern North America.

For all sites studied, the column stress ratios predicted by static and response spectrum methods compare very well

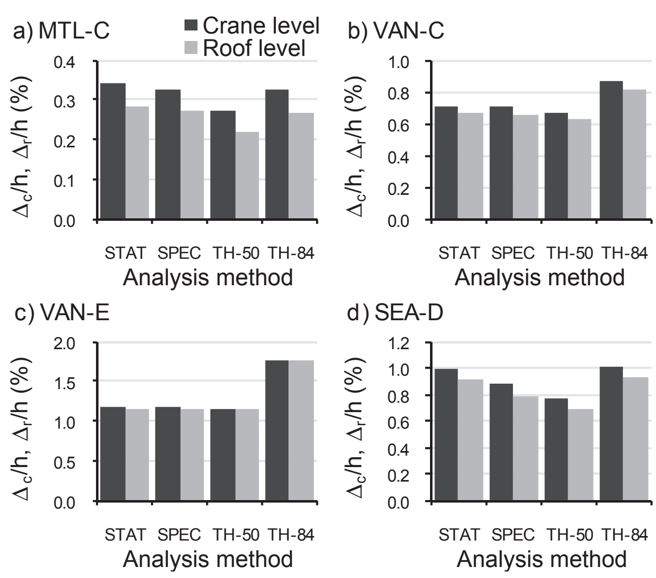

Fig. 6. Peak horizontal displacements from equivalent static (STAT), response spectrum (SPEC) and time-history (TH-med and TH-84th) analysis methods.

with the median values obtained from time-history analysis (Figure 8). The only noticeable difference is observed for the exterior base column in the Seattle frame (about 15% overprediction). The variability of earthquake records has a more pronounced effect on the response of the Vancouver frames, as can be seen from the 84th percentile results. The high stress ratio values in Figure 8 under the seismic effects reduced by force modification factors $R_dR_o = 1.95$ or $R = 3.0$ suggest that the demand from design-level earthquakes will, in fact, exceed the column capacities. This in itself is not a major concern as long as the level of ductility implicitly assumed in design can be effectively provided. This aspect is examined further next.

Assessment of Inelastic Demand

No explicit ductility capacity or strength hierarchy checks were performed in design because the structural systems selected are of the low-ductility category. For these systems, it is expected that the lower seismic force modification factors considered in design would translate into limited and uniformly distributed inelastic demand. It was thus of interest to examine the amplitude and distribution of the expected inelastic response and evaluate the potential for nonductile member failure modes that can detrimentally affect the structural integrity. For this purpose, the peak seismic force demands on the columns from the elastic dynamic time-history analyses described earlier were combined with the member forces from gravity loads. The stress ratios were computed at the expected strength level, i.e., with member resistances determined with a resistance factor of 1.0 and expected steel yield strength, R_yF_y, equal to 1.1 times the nominal value. Note that the forces from time-history analysis are not divided by the force modification factors, as was done previously, such that the seismic force demand corresponds to the design earthquake level.

The computed median and 84th percentile stress ratio values are illustrated in Figures 9, 10 and 11 for the two Vancouver sites and Seattle, respectively. The stress ratios for the Montreal building were less than 1.0 (the columns would remain elastic), and the results for this structure are not discussed further. The values presented are the maximum values obtained for the different limit states and for both sides of the buildings. For the Vancouver frame on firm ground (VAN-C, Figure 9), the columns are expected to remain elastic at the median demand level, but the capacity of three members is exceeded under the 84th percentile force demand. The base of the exterior column was identified as the most critical location (26% overload). The situation is more critical for the VAN-E case: the base of the exterior column (29% overload), the upper column segment (31% overload) and diagonal members in the upper part of the laced column are expected to sustain inelastic demand under the 50th percentile seismic demand. These results are not surprising because the seismic load combinations governed the design of the same members for that structure and system ductility was accounted for in design. For this site, nearly all column members are overstressed under the 84th percentile force level, and the maximum demand-to-strength ratio (252%) is observed at the base of the exterior column. In Figure 11, the results for the Seattle site are similar to the ones obtained

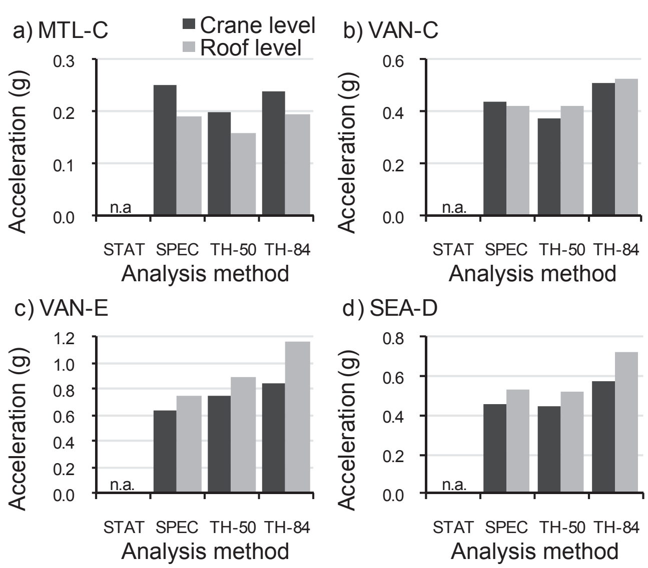

Fig. 7. Peak horizontal accelerations from equivalent static (STAT), response spectrum (SPEC) and time-history (TH-med and TH-84th) analysis methods.

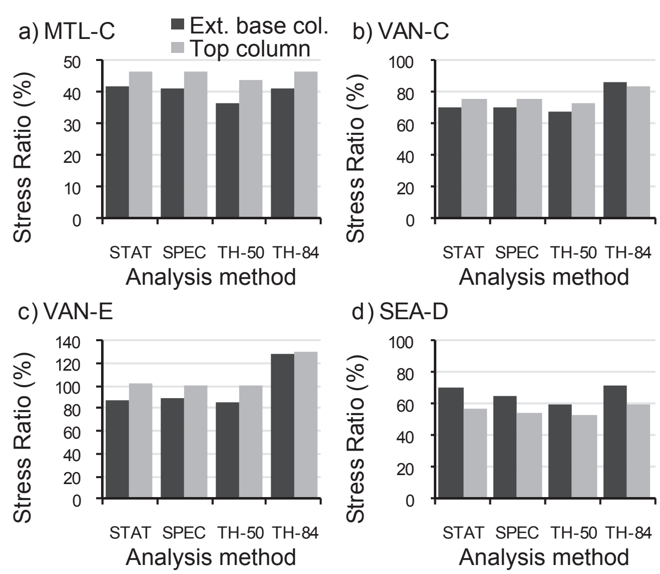

Fig. 8. Peak column stress ratios from static (STAT), response spectrum (SPEC) and time-history (TH-med and TH-84th) analysis methods.

for the VAN-C site at the base of the laced column. However, the demand on the upper column segment is reduced. It is noted that that the time-history analysis for Seattle was performed under the design-level ground motions. Higher demand would be expected under the maximum credible earthquake (MCE) level typically used for assessing seismic performance (1.5 times higher).

The ductility capacity associated with column failure depends on whether bending moments or axial loads dominate the seismic force demand. Figure 12a illustrates the axial load-bending moment demand at the base of the exterior column for the VAN-C case under a ground motion recorded during the 1989 Loma Prieta earthquake. The interaction equations for cross-section strength and in-plane buckling are illustrated in the figures. Both interactions are based on expected member strength with $\phi = 1.0$ and $R_y F_y = 1.1 F_y$. As shown, the seismic demand is highly dominated by axial load due to the cantilevered truss action that develops under lateral loads, and column instability failure is predicted, regardless of whether single or double curvature ($\kappa = -1$ or $+1$) is assumed in the interaction equations. The same response was observed in all other cases studied, suggesting that column buckling, a failure mode that exhibits limited ductility, is likely to occur at the base of the laced columns in these structures. Conversely, the building seismic response induces highly variable in-plane bending moments in the upper column segment while the axial load remains nearly constant (Figure 12b). Verification of the interaction equations at every time step indicates that failure will likely develop on the form of lateral-torsional buckling, rather than by in-plane flexural yielding, suggesting limited ductility capacity. Ductile in-plane flexural hinging response of the upper column segment could be achieved by adding lateral bracing.

SEISMIC DESIGN AND RESPONSE OF THE IRREGULAR BUILDING

Building Studied and the Analysis Model

A three-dimensional view of the heavy industrial building selected for this study is shown in Figure 13a. It is an existing structure located near Montreal, Canada, that houses a vertical mechanical titanium refinement process. The geometry, mass and stiffness distribution are highly irregular. The layout of the columns at the base of the building is illustrated in Figure 13b. The main portion of the building has 37-m by 59-m (121-ft by 194-ft) plan dimensions and is 43 m (141 ft) high. An 8-m (26-ft) tall penthouse is located in the southwest part of the structure. The building also includes two extensions, one in the northwest corner (5 m by 6 m [16 ft by 20 ft]; 18 m [59 ft] high) and one in the southeast corner (24 m by 8 m [79 ft by 26 ft]; 6 m [20 ft] high). Figure 13a shows a recent addition to the south of column line 11. That addition is not illustrated in subsequent figures and was not considered in the study. Several platforms supporting different equipments are concentrated in the south and

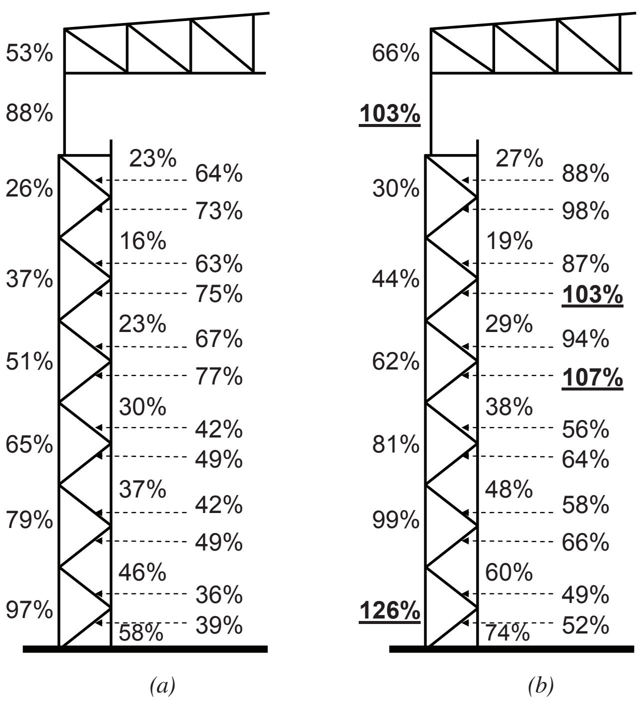

Fig. 9. Stress ratios for the VAN-C frame using expected member resistance: (a) median values; (b) 84th percentile values.

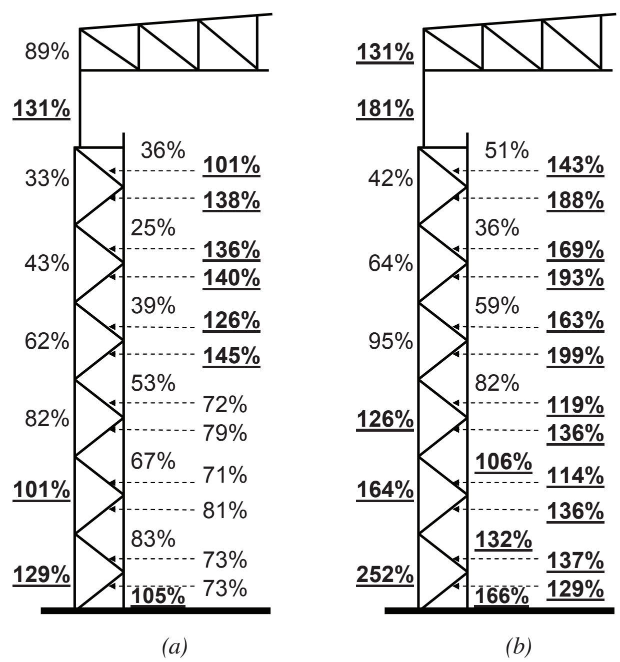

Fig. 10. Stress ratios for the VAN-E frame using expected member resistance: (a) median values; (b) 84th percentile values.

north portions of the building, leaving a large open space in the center that extends almost throughout the whole building height. The building also houses two large-capacity silos (750 t and 1200 t [830 T and 1300 T]) between lines 1 and 4, as well as other smaller pieces of equipment located throughout the structure. Lateral loads are primarily resisted by concentrically braced steel frames located at the perimeter of the building. Additional braced frames are provided in the vicinity of the heavy equipment and large openings.

The existing design served as a start-off point to build the three-dimensional numerical model shown in Figure 14. Some simplifications were made to obtain results that could be indicative of the behavior of similar buildings of this type and not only of the particular building studied. The model was created using the program STAAD.Pro (Bentley, 2008) and includes columns, beams, horizontal bracing and vertical braced frames. The members providing support for the main equipments were also included. Although all

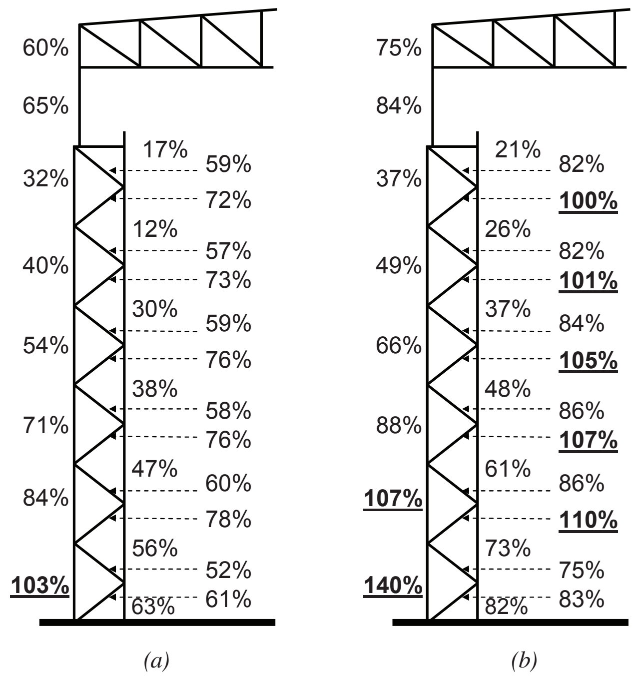

Fig. 11. Stress ratios for the SEA-D frame using expected member resistance: (a) median values; (b) 84th percentile values.

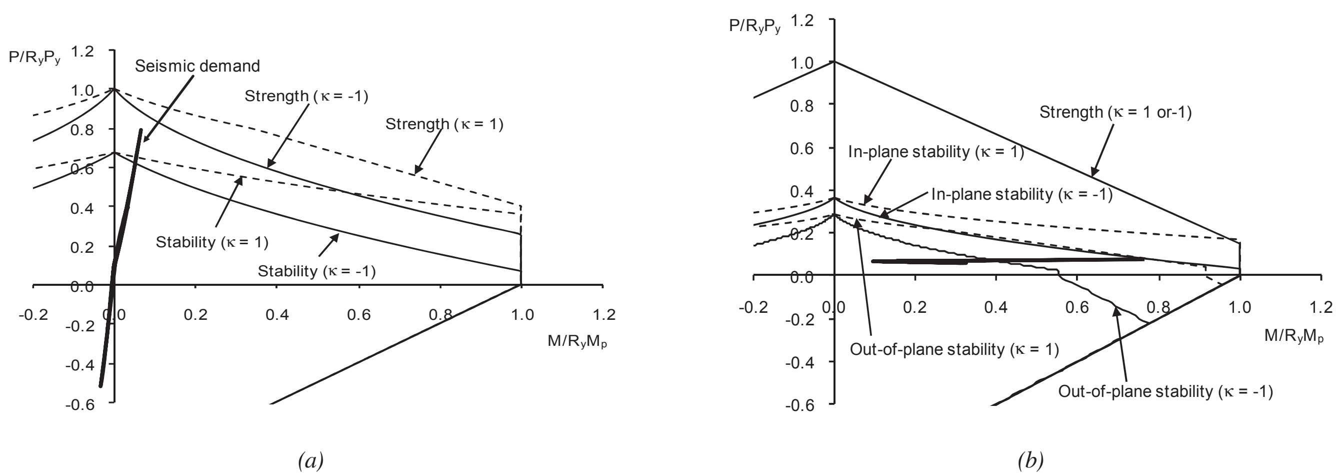

Fig. 12. Axial load-bending moment seismic demand under the Loma Prieta ground motion record versus expected member resistance of the exterior column of the VAN-C building: (a) at the base of the lower column segment; (b) at the base of the upper column segment (axial compression is positive in the graph).

the platforms were included in the model, rigid diaphragm properties were considered only for the floors with a concrete slab. The floor arrangement is illustrated in Figure 14a; the four perimeter braced frames that will be examined later are illustrated in Figure 14b.

The total seismic weight of the structure ($W = 74{,}200$ kN = 16,700 kips) was determined in accordance with NBCC 2005 and includes the weight of the structural members, 25% of the roof snow load and the weight of the main pieces of equipment in the fully loaded condition. As in the crane-supporting structure, the seismic weight was distributed at every node of the structure model. In view of their importance and nonuniform distribution, the masses of the major equipments were assigned to additional nodes positioned at the center of gravity of the equipment and linked to the rest of the structure with very stiff members. By doing so, local overturning moments due to the horizontal inertia forces acting above the base of the equipments could be incorporated in the analyses. The masses of the remaining equipment were assigned to the supporting columns at each floor in proportion to their tributary areas.

Validation of Seismic Analysis Methods Used in Design

Seismic load effects were first determined using the equivalent static and response spectrum analysis methods. Selected response parameters were then compared to values obtained from elastic time-history analysis to validate the application of current seismic design procedures to irregular industrial buildings. According to NBCC 2005, dynamic analysis, either spectral or time history, is mandatory for such a highly irregular building. Nevertheless, the equivalent static method is also considered; it is much simpler to use at the preliminarily design phase and is commonly employed by practicing engineers for this purpose. The study was done for the class C site in Montreal for consistency with the existing design. The elastic design spectrum shown in Figure 3 and the ensemble of 14 synthetic accelerograms previously described for the crane-supporting building at the MTL-C site were then applied again herein. In the static and response spectrum analysis methods, the force modification factors R_dR_o were set equal to 1.0 for direct comparison with time-history analysis. For simplicity, accidental torsion was ignored in the calculations, and gravity loads were not included in the model. Consequently, P-delta effects were neglected in the analyses.

The fundamental periods were computed first using the Rayleigh method: 1.29 and 1.28 s in the E-W and N-S directions, respectively. Modal analysis was then performed for verification and the results are presented in Table 2. The analysis confirmed that the two principal modes of the building were in the orthogonal directions, with periods equal to 1.38 and 1.32 s in the E-W and N-S directions, respectively. Both directions had strong torsional components. Period estimates from the NBCC empirical formula for braced frames, $T_a = 0.025\,h$, with h in meters, are also in good agreement with the Rayleigh and modal periods: T_a = 1.08 s when $h = 43$ m (141 ft) is used and T_a = 1.28 s with h = 51 m (167 ft) at the penthouse location. The NBCC allows

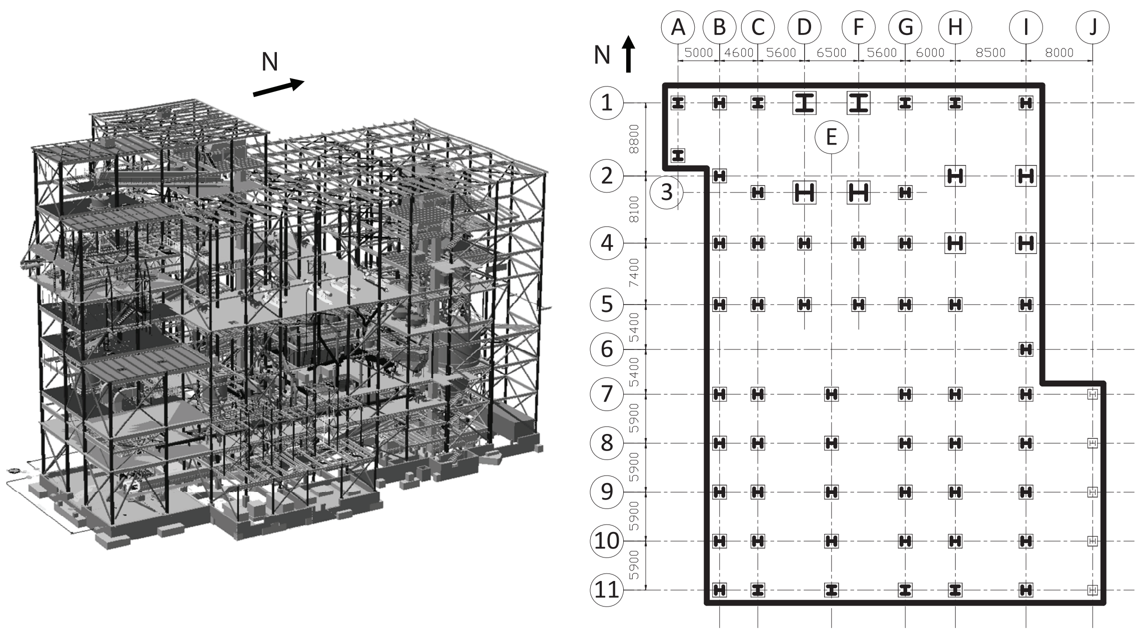

(a) (b)

Fig. 13. Irregular building studied: (a) three-dimensional view; (b) column layout at the base.

periods up to 2.0 times T_a when justified by modal analysis.

Elastic values of the base shear forces from the equivalent static method, V, were determined using the periods from the Rayleigh method: 8900 kN (2000 kips) and 9000 kN (2025 kips) along the E-W and N-S directions, respectively. As shown in Table 2, the masses associated with these two fundamental modes only correspond to 53 and 63% of the total mass. In comparison, the mass associated with higher modes is small (less than approximately 7% each). For the response spectrum analysis, a total of 70 modes had to be considered for the E-W direction and 95 modes for the N-S direction in order to obtain the 90% mass participation required by codes (see Table 2). The resulting base shear forces V_t are equal to 5690 kN (1280 kips) and 6460 kN (1450 kips) in the E-W and N-S directions, respectively, i.e., corresponding to only 64 and 72% of the equivalent static method values, respectively. As was the case for the mill-type building, the equivalent static method is found to provide conservative estimates of the force demand. By including up to 126 modes, the combined mass participation increases to 97 and 96% in each of the two directions (see Table 2) and the two associated base shear forces increase to 71 and 79% V, respectively. Similarly to the mill-type building, further increasing the number of modes did not lead to any further enhancement of the response spectrum analysis base shears, and the remaining differences between V_t and V could be attributed to the inability of the static method to adequately represent the dynamic response of complex structures. In this context, the need to scale response spectrum analysis results to values obtained by equivalent static method could be questioned when the number of modes used in the spectral analysis is sufficient to reach convergence; however, this would necessitate further investigation. Herein, the results of the first response spectrum analysis based on 90% participating mass were scaled by the V/V_t ratio, as required in NBCC 2005 provisions, and then used for the comparison with other methods. The force demand from the equivalent static method was obtained from two seismic load profiles in order to assess the approach for inclusion of higher modes: (1) the linear distribution with concentrated force at the top of the structure prescribed in NBCC 2005 and (2) the parabolic distribution as defined in ASCE 7-05.

Three-dimensional dynamic time-history analysis was carried out using the modal superposition routine available in the program STAAD.Pro. Damping equal to 5% of the critical value was assigned in all modes. Preliminary analyses were performed to determine the appropriate number of modes required to adequately predict the seismic base shear, story displacements and maximum brace forces. The number of modes was gradually increased to achieve 90% (70 modes in E-W direction, 95 modes in N-S direction), 97% (126 modes) and ±100% (500 modes) participating mass. Increasing the participating mass from 90 to 97% resulted in peak base shear forces increasing by as much as 25%; however, no further base shear increase was observed beyond 126 modes. Similarly, brace maximum forces changed significantly until 126 modes were included, and the results remained constant when additional modes were considered. Story displacements were the least sensitive to the number of modes selected; however, for specific building levels, it was necessary to solicitate 97% of the mass to avoid changes in the results. Based on these three observations, 126 modes were selected for all time-history analyses. In view of the number of selected accelerograms, median results from time-history analysis can be considered as representative, but 84th percentile values were also tracked to illustrate

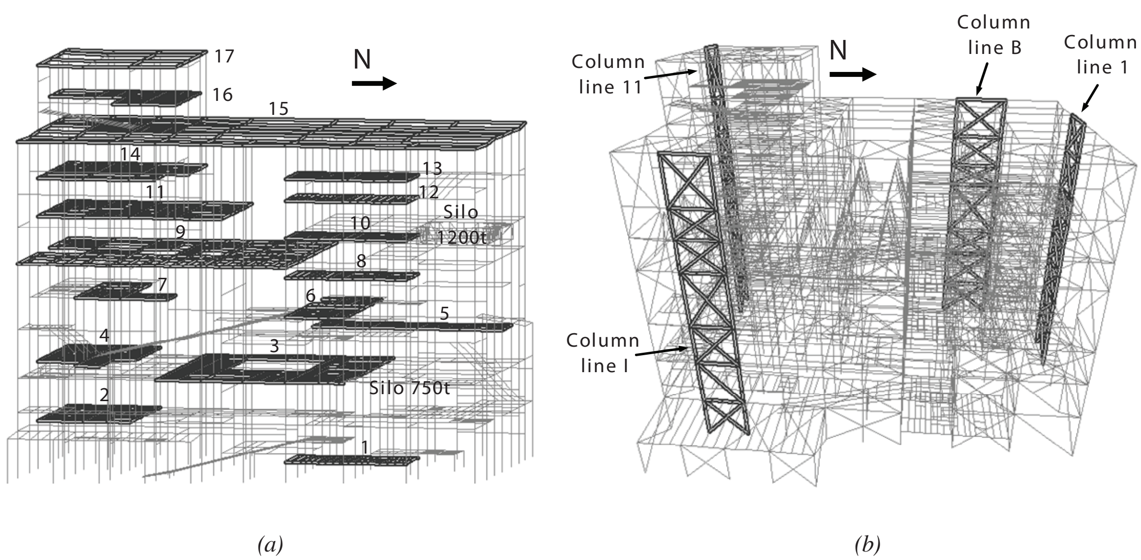

Fig. 14. Building floors and braced frames studied: (a) location of floors; (b) elevation of the braced frames studied.

Table 2. Modal Properties of the Irregular Building Along the Building Orthogonal Directions					
Mode	T_i s	E-W		N-S	
		M_i %	$\Sigma M_i/M$	M_i %	$\Sigma M_i/M$
1	1.46	0.0	0.0	0.2	0.2
2	1.38	53.2	53.2	2.1	2.1
3	1.32	1.5	54.7	63.4	65.7
4	1.11	0.2	54.8	0.2	65.9
5	1.07	7.1	62.0	0.0	65.9
6	1.05	4.2	66.2	0.2	66.1
7	1.02	0.0	66.2	0.0	66.1
8	0.98	3.8	70.0	0.7	66.9
9	0.96	0.7	70.7	5.1	72.0
…	…	…	…	…	…
70	0.38	0.1	90.0	0.1	86.2
…	…	…	…	…	…
95	0.33	0.5	92.9	0.4	90.3
…	…	…	…	…	…
126	0.26	0.3	97.1	0.1	96.1

dispersion. The analyses were conducted for two sets of orthogonal axes: the principal axes of the building and the set of axes oriented at a 45° angle with respect to the principal axes. The latter set was selected to evaluate the impact that the direction of the analysis may have on the response. Three response parameters provided bases for comparison between the different analysis methods, namely, the seismic base shear, story displacements and the axial forces in columns and braces of the selected perimeter braced frames illustrated in Figure 14b. The results are presented in Figures 15, 16 and 17, respectively.

Figure 15 shows that similar base shear values were obtained in two principal building directions. This result was expected because the corresponding building periods in two directions are very close. Elastic design shears were approximately 40% higher compared to median values of time-history results, and even slightly exceeded the maximum values obtained from time-history analysis. Note that median results are in good agreement with results obtained from response spectrum analysis when no scaling of base shear is applied, confirming the conservatism of the static force demand based on fundamental mode response.

Figure 16 shows calculated peak displacements for loads and ground motions applied in the N-S direction. The displacements were normalized by the story height measured from ground. All employed methods predicted comparable displacement profiles. For the equivalent static method, very little difference was observed between the results obtained when using the NBCC 2005 and ASCE 7-05 load distributions. Spectral values were slightly smaller than those obtained for equivalent static load profiles in all but two locations and about 40% higher than the mean values from time-history analysis. Eighty-fourth percentile results were also below the predictions of the equivalent static and response spectrum methods. These observations are consistent with those made for the base shear.

Figure 17 compares column and brace axial load profiles in the selected braced frames for earthquake action along the N-S direction of the building. Results obtained for E-W load application showed similar trends. In general, for the columns and diagonals studied, all methods resulted in similar force profiles. The response spectrum analysis values are consistently higher compared to median time-history results and even exceed the 84th percentile time-history values for almost all elements studied. This is not surprising in view of the scaling procedure that was applied to the response spectrum analysis results. The results obtained with the static equivalent method are comparable to response spectrum values for the frames oriented in the direction of the analysis. For the frames in the perpendicular direction, however, the equivalent static method underpredicted the member forces by a large margin in some cases. This can be attributed to the inadequate inclusion of higher mode effects and the effects of torsion when equivalent static method is used for such an irregular structure.

It was of further interest to see if the direction of the application of the load can affect response forces. Figure 18 summarizes results obtained for four directions of load application: along the two principal directions of the building and along the two orthogonal axes oriented at a 45° angle with respect to the building principal axes. Force envelopes obtained from the response spectrum analysis are also shown for comparison. The reader is reminded that column lines B and I run in the N-S direction, while column lines 1 and 11 are in the E-W direction. It would normally be expected that the highest forces in columns and braces are induced when the load is applied in the direction of the braced frame. In Figure 18, this is indeed the case for the braces of all frames studied. However, in the upper columns of the frames along the E-W direction, up to 30% higher forces are observed when the ground motion is applied in directions other than the direction parallel to the frames, including loading at 45°. This is attributed to the fact that these columns are also part of other braced frames (not studied herein) acting in the perpendicular direction. This situation is not unusual in industrial buildings of this type, and the results indicated that caution should be exercised when selecting the direction of the seismic loading. For such columns, NBCC requires that forces from members framing into the columns from all directions be considered in design. In ASCE 7, columns that form part of two intersecting systems must be designed for ground motions applied in any directions, but only if the structure is assigned to Seismic Design Categories D or E. In all cases studied, the member forces obtained from response spectrum analysis were the highest and would thus provide conservative estimates of design forces.

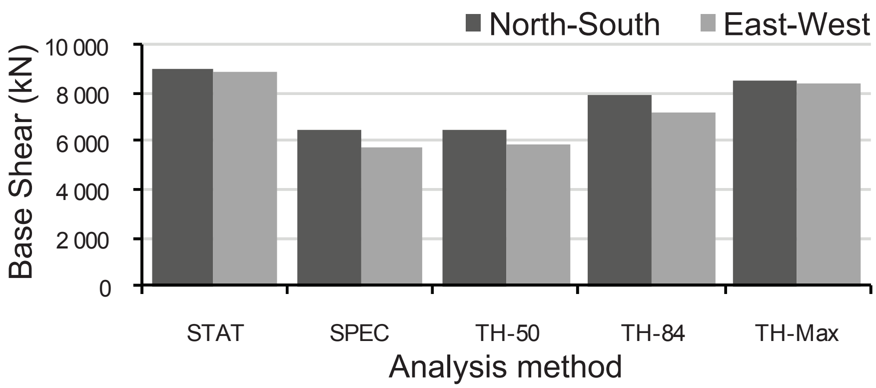

Fig. 15. Peak base shear from equivalent static (STAT), response spectrum (SPEC) and time-history (TH-med and TH-84th) analysis methods (1 kip = 4.45 kN).

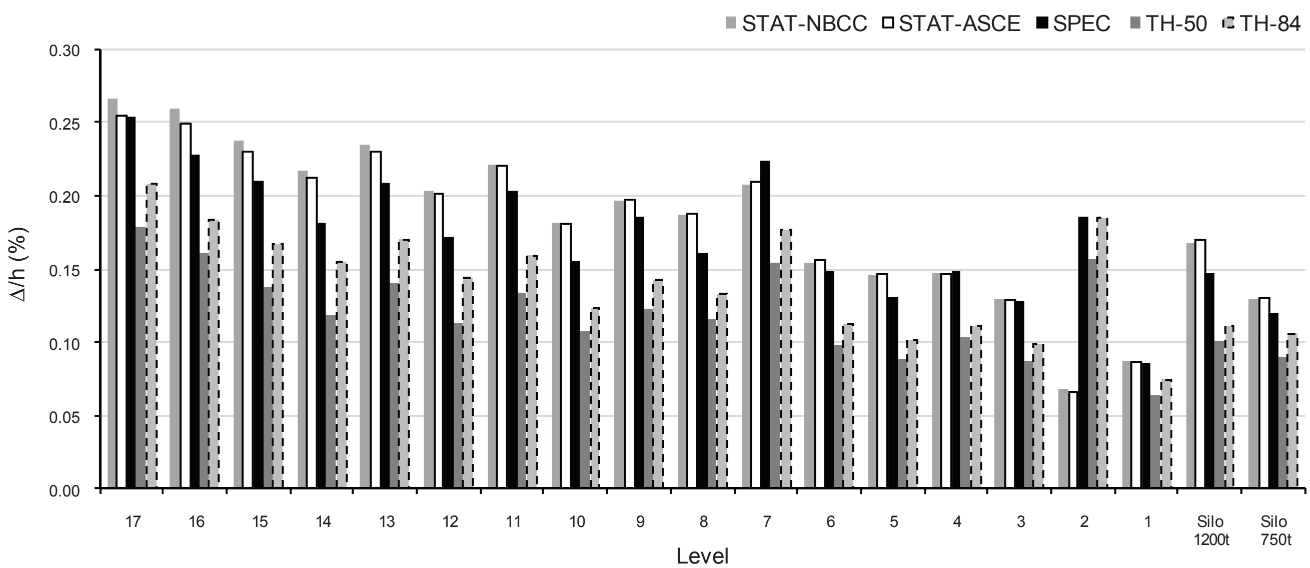

Fig. 16. Peak drift from equivalent static (STAT), response spectrum (SPEC) and time-history (TH-med and TH-84th) analysis methods and for earthquake action along the N-S direction.

CONCLUSIONS AND FINAL COMMENTS

Elastic time-history dynamic analyses were performed for two different types of industrial buildings to validate the predictions from the equivalent static force procedure and the response spectrum analysis method prescribed in current building codes. The first building studied was a typical crane-supporting, mill-type building. The study was carried out for four different sites representative of typical eastern and western North American seismic conditions. The second building is an existing tall structure that is highly irregular in geometry, mass and stiffness distribution. Its seismic response was studied only for the Montreal site for consistency with the original design. The structures as designed do not meet the restrictions imposed in current (2005) building codes; the height of the buildings exceed the 15-m (50-ft) limit imposed in the National Building Code of Canada for steel seismic force-resisting systems of the conventional construction category, and $R = 3.0$ as used for the design of the building in Seattle is not permitted for building structures according to ASCE 7.

For both structures, the fundamental periods of vibrations from code empirical formulas compared well with

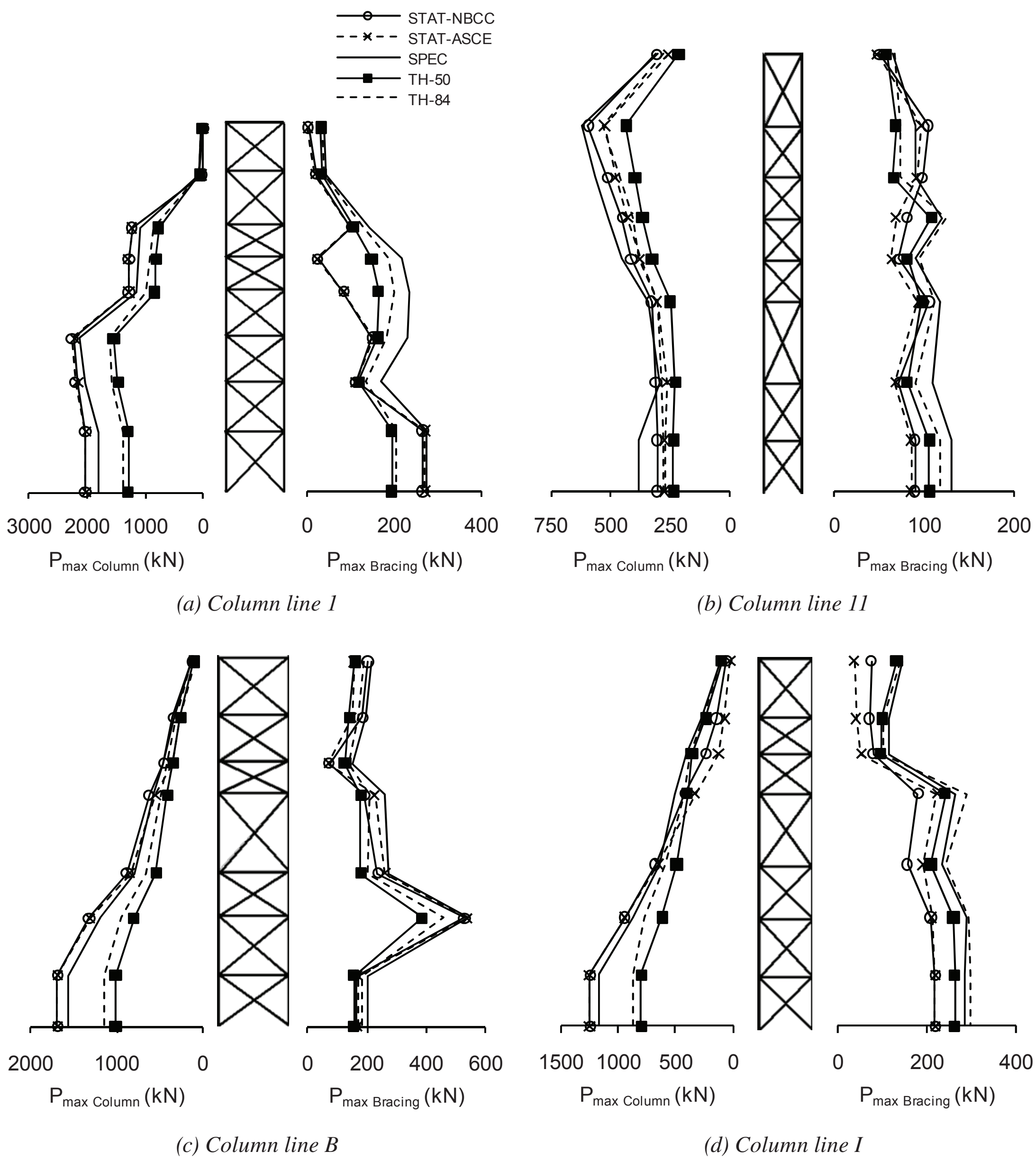

Fig. 17. Peak axial load in columns and bracing members from equivalent static (STAT), response spectrum (SPEC) and time-history (TH-med and TH-84th) analysis methods for earthquake action along the N-S direction (1 kip = 4.45 kN).

the periods obtained from modal analysis. For the irregular structure, good period match was also obtained when using the Rayleigh method. The equivalent static force procedure static method consistently gave higher values of the total earthquake force, or base shear, compared to the response spectrum analysis method when the number of modes considered in the latter was set to obtain 90% combined mass participation, as prescribed in codes. This effect on the global seismic demand is corrected when applying the scaling procedures prescribed in codes. For the structures studied, no further significant change in the base shear obtained by response spectrum analysis was observed when the number of modes considered increased beyond the one required to obtain in the order of 96 to 97% participating mass. Therefore, it is recommended to adopt a tighter criterion in response spectrum analysis, prior to scaling to equivalent static values, to better represent the complex dynamic response of these structures, especially for tall and irregular buildings such as the one examined herein.

For the crane-supporting building, the horizontal displacements from both code analysis methods are similar and agree well with the median demand from seismic ground motions. Except for the Montreal site, the drifts at the crane level exceeded the limit recommended to prevent damage

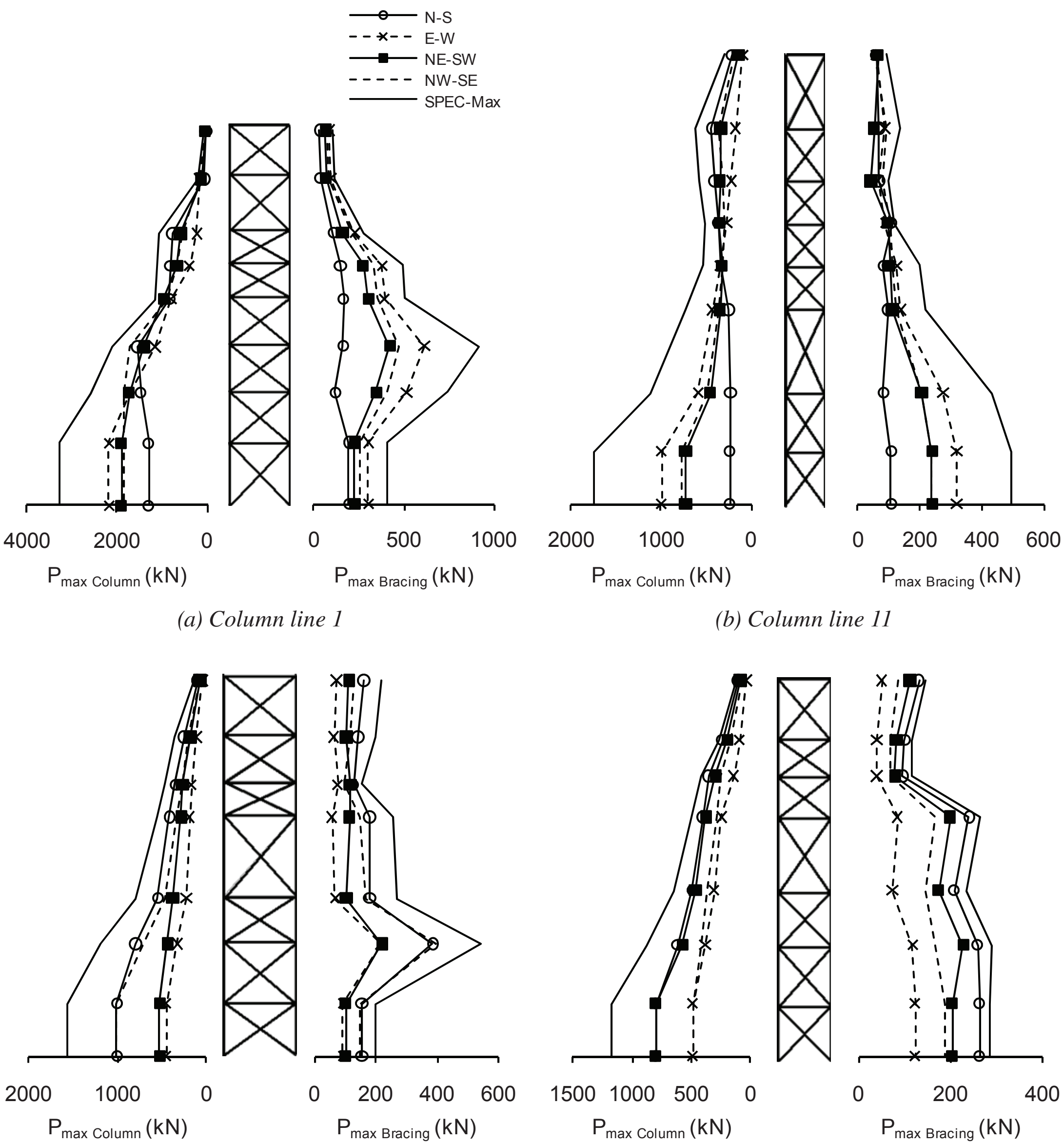

Fig. 18. Peak axial load in columns and bracing members from time-history and response spectrum analysis methods (1 kip = 4.45 kN).

to the lifting equipment in this building type. Median peak horizontal accelerations from dynamic analysis are well predicted by response spectrum analysis. Seismic force demand governed the design of the upper column segment, individual column members at the base of the laced column segment and lacing members. For the column members, the static and response spectrum analysis methods predicted well the median force demand obtained from time-history analyses. That force demand was found to exceed the expected member strengths, at both the 50th and 84th percentile levels, indicating that inelastic column behavior may occur in these structures. This response is a consequence of the force modification factors used in design and was expected. However, the study also showed that stability limit states would govern the inelastic column response. The ductility capacity associated with such inelastic behavior can be limited, and can possibly be less than that implicitly assumed in design, with potential detrimental impact on the structural integrity in case of strong earthquakes.

The study of the irregular building showed that the equivalent static method can be used to estimate displacements, but may lead to unconservative predictions of column and brace forces. In all cases studied, regardless of the direction of the analysis, response spectrum analysis also resulted in higher force demand compared to elastic time-history analysis. Scaling requirements prescribed in codes likely contributed to this conservatism. Nevertheless, the method appears to be very appropriate to predict the seismic response of such highly irregular structures. If dynamic time-history analysis is performed using a modal superposition technique, as was done in this study, the results showed that element forces are sensitive to the number of modes considered and can be significantly underestimated if an insufficient number is selected. For the building studied, the number of modes for obtaining 97% global mass participation was needed to adequately predict the base shear force demand. The study also showed that the selection of the direction in time-history analysis should be done with care, because the maximum forces in elements that are part of two orthogonal-braced frames are not always induced by seismic loads acting in the direction parallel to the bracing systems.

The results presented in this paper were obtained for a limited number of structures and cannot be fully generalized. Further studies on additional structures should be performed to validate the findings of this research. However, the results provide insight into possible limitations of current seismic design procedures and possible directions for future investigation. For instance, one could study the need for scaling the results from response spectrum analysis to the equivalent static values when a sufficient number of modes are considered in the response spectrum analysis. Modal superposition time-history analyses, with constant damping ratios in all modes, were performed in this study, which may result in conservative predictions of the higher-mode effects. Comparison should be made with direct integration techniques and Rayleigh damping models. Nonlinear time-history analyses should be carried out to better assess the inelastic demand imposed on critical members and connections of industrial buildings and evaluate the effects of this inelastic response. Physical testing should be conducted to assess the ductility capacity associated with the governing limit states that are predicted by analysis. For mill-type buildings, this study suggests that column buckling is a possibility: out-of-plane of the frame for the upper column segment and in-plane for the base columns. In case the available ductility is found to be inadequate, techniques should be examined to enhance the inelastic seismic column response (e.g., minimum bracing requirements to prevent out-of-plane buckling of the upper columns or ductile fuse systems to control the axial force demand in the base column members).

ACKNOWLEDGMENTS

This project was funded by the Natural Sciences and Engineering Research Council (NSERC) of Canada and Hatch Ltd. (Consulting Engineering). The authors express their appreciation to Robert A. MacCrimmon of Hatch Energy, Niagara Falls, Canada, for his most valuable input in the selection and design of the structures studied.

REFERENCES

AISC (2005), *ANSI/AISC 360-05, Specification for Structural Steel Buildings,* American Institute of Steel Construction, Chicago, IL.

AISE (2003), *Guide for the Design and Construction of Mill Buildings*, *AISE Technical Report No. 13,* Association for Iron and Steel Technology, Pittsburgh, PA.

ASCE (2005), *ASCE/SEI 7-05, Including Supplement No. 1, Minimum Design Loads for Buildings and Other Structures,* American Society of Civil Engineers, Reston, VA.

ASCE (2010), *ASCE/SEI 7-10, Minimum Design Loads for Buildings and Other Structures,* American Society of Civil Engineers, Reston, VA.

Bendimerad, F., Johnson, L., Coburn, A., Rahnama, M. and Morrow, G. (1999), *Kocaeli, Turkey Earthquake*—Event Report, Risk Management Solutions, Inc., Menlo Park, CA.

Bentley (2008), *STAAD.Pro. Version 20.07.03.16.* Bentley Systems, Inc., Yorba Linda, CA.

CSA (2001), *CAN/CSA-S16-01 Limits States Design of Steel Structures*, *Including CSA-S16S1-05 Supplement No. 1,* Canadian Standards Association, Willowdale, ON, Canada.

Daali, M. (2004), "Industrial Facilities and Earthquake Engineering," *Proc., 13th World Conference on Earthquake Engineering,* Vancouver, BC, Canada, Paper No. 330.

Fisher, J.M. (2004), *Design Guide 7 Industrial Buildings, Roofs to Anchors Rods*, 2nd ed., American Institute of Steel Construction, Chicago, IL.

Humar, J., Adams, J., Tremblay, R., Rogers, C. and Halchuk, S. (2010), "Proposals for the Seismic Design Provisions of 2010 National Building Code of Canada," *Proc. 9th US National and 10th Canadian Conference on Earthquake Engineering*, Toronto, ON, Canada, Paper No. 1387.

Johnson, G.S., Ascheim, A. and Sezen, M. (2000), "Industrial Facilities," *Earthquake Spectra*, Vol. 16, No. S1, pp. 311–350.

NRCC (2005), *NBCC 2005.* National Building Code of Canada. National Research Council of Canada, Ottawa, ON, Canada.

MacCrimmon, R.A. (2004), *Guide for the Design of Crane-Supporting Steel Structures,* Canadian Institute of Steel Construction, Toronto. ON, Canada.

Rahnama, M. & Morrow, G. (2000), "Performance of Industrial Facilities in the August 17, 1999, Izmit Earthquake," *Proc. 12th World Conference on Earthquake Engineering,* Auckland, New Zealand.

Richard, J. (2009), Étude du comportement sismique de bâtiments industriels avec systèmes de contreventement de faible ductilité, M.Sc. Thesis, École Polytechnique, Montréal, QC, Canada (in French).

Rolfes, J.A. & MacCrimmon, R.A. (2007), "Industrial Building Design—Seismic Issues," *Iron and Steel Technology,* Vol. 4, No. 5, pp. 282–298.

Schmidt, J.A. (2001), "Design of Mill Building Columns Using Notional Loads," *Engineering Journal*, AISC, Vol. 39, No. 2, pp. 90–99.

Sezen, H., Elwood, K.J., Whittaker, A.S., Mosalam, K.M., Wallace, J.W. and Stanton, J.F. (2000), "Structural Engineering Reconnaissance of the August 17, 1999, Kocaeli (Izmit), Turkey, Earthquake," PEER Report No. 2000/09, PEER Center, University of California, Berkeley, CA.

Swan, S.W. and Hamburger, R. O. (1991), "Industrial Facilities," *Earthquake Spectra*, Vol. 7, No. S2, pp. 49–58.

Swan, S.W., Wesselink, L., Bachman, R.E., Malik, L., Eli, M. and Porush, A. (1990), "Industrial Facilities," *Earthquake Spectra*, Vol. 6, No. S1, pp. 189–238.

Thiel, C. (Ed.) (1986), "The Chile Earthquake of March 3, 1985—Industrial Facilities," *Earthquake Spectra*, Vol. 2, No. 2, pp. 373–409.

Tremblay, R. Timler, P., Bruneau, M. and Filiatrault, A. (1995), "Performance of Steel Structures During the 1994 Northridge Earthquake," *Canadian Journal of Civil Engineering,* Vol. 22, No. 1, pp. 338–360.

Tremblay, R., Bruneau, M., Driver, R., Metten, A., Montgomery, C.J. and Rogers, C. (2010), "Seismic Design of Steel Structures in Accordance with CSA-S16-09," *Proc. 9th US National and 10th Canadian Conference on Earthquake Engineering*, Toronto, ON, Canada, Paper No. 1768.

Yanev, P. (1989), "Performance of Industrial Facilities," *Earthquake Spectra*, Vol. 5, No. S1, pp. 101–113.